

Scaling accretion flow models from BHB to AGN

– Why doesn't it work? –

Chris Done¹

¹ Department of Physics, University of Durham, South Road, Durham DH1 4ED

E-mail(CD): chris.done@durham.ac.uk

ABSTRACT

Black holes depend only on mass and spin, while what we see from the accretion flow in steady state depends also on mass accretion rate and (weakly) inclination. Hence we should be able to scale the accretion flow properties from the stellar to the supermassive black holes. But the data show significant differences between these two types of systems, suggesting that we are missing some crucial physics in AGN. One of these differences is the soft X-ray excess which is seen ubiquitously in bright AGN, but only occasionally in BHB. Another is the much faster variability seen in the high energy tail of high mass accretion rate AGN compared to that seen in the tail of BHB. We show that while this variability is not understood, it can be used via the new spectral-timing techniques to constrain the nature of the soft X-ray excess. The coherence, lag-frequency and lag-energy results strongly support this being an additional low temperature Comptonisation component rather than extreme relativistically smeared reflection in the 'simple' Narrow Line Seyfert 1 PG1244+026.

KEY WORDS: Accretion flows: Black holes: Binaries: Active Galactic Nuclei

1. Introduction

Understanding accretion in strong gravity is a challenge, so we need to use all available information to build up a physical picture of what happens. The black hole binaries (BHB) give an observational template of how the accretion flow varies as a function of (mostly) $\dot{m} = L/L_{Edd}$, which we can then scale up to the supermassive black holes in Active Galactic Nuclei (AGN) to predict how we expect AGN to behave. Any differences between these models and the data mean that there are some aspects which do not simply scale with mass, giving insight into the additional physical processes required.

2. Black hole Binaries

In BHB the overall spectral and timing properties can all be fit into a model where the standard disc extends down to the last stable orbit only at high L/L_{Edd} . At luminosities below $L \sim 0.02L_{Edd}$ the optically thick, geometrically thin inner disc progressively recedes, probably via evaporation (Meyer & Meyer-Hofmeister 1994; Mayer & Pringle 2007) and is replaced by a hot, probably radiatively inefficient, optically thin, geometrically thick flow. The characteristic hard X-ray spectrum and variability are (mostly) generated in the flow, with the longest variability timescales set by the outer radius of the flow. As the disc recedes, this outer flow size increases, so all the timescales increase (including the QPO which may be a

sign of vertical precession of the entire hot flow: Ingram & Done 2012). The drop in disc seed photons means that this correlates with a decrease in direct disc emission, and with increasing spectral hardness of the high energy tail (see e.g. the reviews by Remillard & McClintock 2006; Done, Gierlinski & Kubota 2007).

Transition spectra are complex, with strong disc and strong coronal emission. The corona is also probably inhomogeneous, with softer compton spectra emitted in the outer regions of the flow which is closer to the disc, and harder spectra in the inner regions which intercept less disc emission. Signatures of this are that the compton emission has complex time lags associated with it. Photons at higher energies are correlated with those at lower energies, but with a (frequency dependent) lag time (Miyamoto & Kitamoto 1989; Nowak et al 1999). This can be modelled by each part of the flow generating variability on a timescale which decreases with radius, and where variability at each radius propagates down through the accretion flow to modulate the variability at smaller radii (Kotov et al 2001; Arevalo & Uttley 2006; Ingram & Done 2012; Axelsson et al 2014).

At very high luminosities the spectra can also be similarly complex, with a strong disc and strong soft compton tail (Belloni et al 2005). These 'very high' or 'steep power law' state spectra may also represent ones where the disc is slightly truncated (Done & Kubota 2006; Tamura et al 2012). However, evaporation is no longer

sufficient to remove the inner disc at these high mass accretion rates, so radiation and/or magnetic pressure (Meier 2005; Machida et al 2006) may play a role.

3. Scale to AGN

AGN live in more complex environments than BHB, so we select only those where obscuration is not an issue. However, scaling from BHB predicts that the intrinsic spectral energy distribution should change similarly dramatically with L/L_{Edd} , unlike the simplest unified AGN models in which obscuration is the only determinant of the observed spectrum. Another difference between AGN and BHB is that the BHB only span a small range in black hole mass (less than a factor of 2) so they form a very homogeneous sample, whereas AGN range from $10^5 - 10^{10} M_{\odot}$. Hence we expect the unobscured AGN spectra to change with both mass and $\dot{m} = L/L_{Edd}$, most obviously as the accretion disc should peak at $T_{disc} \propto (\dot{m}/M)^{1/4}$. This means that the disc typically peaks in the (often unobservable) UV-EUV, so we need multiwavelength data rather than simply using X-ray data to constrain the disc and tail simultaneously as in BHB.

Starting from the BHB, we might then match up some of the different unobscured AGN types to the BHB states. LINERs are at low L/L_{Edd} so may be the analogue of the low/hard state with the inner disc replaced by a hot flow. Seyferts span the transition between the brightest low/hard states and disc dominated states. Quasars are at similar L/L_{Edd} as Seyferts, but with a higher mass black hole giving their higher luminosity. And perhaps the Narrow Line Seyfert 1s are the analogue of the very high state in BHB since these are known to be at high L/L_{Edd} (e.g. Boroson 2002; Woo & Urry 2002). Some evidence for this is that the bolometric correction from the X-ray flux increases substantially with L/L_{Edd} in AGN in a similar way to BHB (e.g. Vasudevan & Fabian 2007).

However, compiling the SED's of these different L/L_{Edd} AGN does not generally support this picture. The only one which seems to work is the LINERs as the analogue of the low/hard state (though even this is somewhat controversial e.g. Maoz 2007 vs Nemmen et al 2014). The lack of an inner disc means no strong UV emission so no broad line region, explaining the optical line ratios which define this class.

But classic Quasar spectra are not disc dominated (as has been known for years, e.g. Elvis et al 1994). Rather than showing clear evidence for a disc which extends down to the last stable circular orbit as in similar L/L_{Edd} BHB, the AGN disc spectra seem to roll over at a lower temperature. They also have hard coronal spectra, with $\Gamma < 2$ in the 2-10 keV band, whereas BHB at this L/L_{Edd} have $\Gamma > 2.2$. Extrapolating this power law

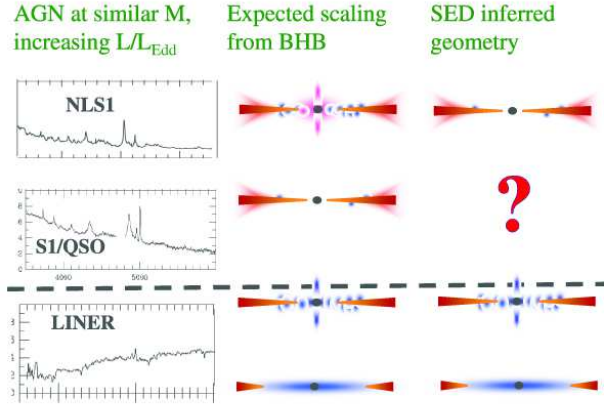


Fig. 1. (left panel) AGN at similar mass but different L/L_{Edd} have different optical line ratios, signalling a change in their SED. (middle panel) The geometries inferred for BHB as a function of increasing L/L_{Edd} , with the dashed black line indicating the collapse of the hot inner flow. (right panel) The observed AGN SED show that while LINERs may well have the truncated disc/hot inner flow of low/hard state BHB, standard broad line Seyferts and Quasars do not look like the disc dominated (or in any other) BHB state. Narrow Line Seyfert 1s at high L/L_{Edd} might be expected to be analogous to the BHB very high state, but their spectra look more like the disc dominated state!

below 2 keV reveals a strong soft X-ray excess - a component which is not apparently seen in disc dominated BHB spectra at these L/L_{Edd} . The origin of this soft X-ray excess is not well understood. Potential models include an additional comptonisation component (e.g. Gierlinski & Done 2004) or extremely smeared reflection (e.g. Crummey et al 2006). However, variability studies on timescales of months suggest that the soft X-ray excess connects to the UV (Mehdipiur et al 2011), while broadband X-ray spectra support models where this component contributes only to the soft X-ray bandpass, and does not extend into the harder band (Matt et al 2014). Together, these point to it being a separate compton component, taking its seed photons from the disc, but having a much lower electron temperature (~ 0.2 keV: Gierlinski & Done 2004) than the high energy Compton tail.

Two Compton components are required in BHB in intermediate states (e.g. Yamada et al 2013), but while these look somewhat similar to the standard Quasar spectra shown here, there is a clear difference. Intermediate type spectra are only rarely seen from BHB as they are clearly only produced in transitions between the two stable types of accretion flow, whereas standard quasars are extremely common, so their spectra cannot represent a rare transition state.

Whatever the origin of the soft X-ray excess, it must be powered by accretion. The mass accretion rate through the outer thin disc sets the total energy available (mod-

ulo black hole spin) and this is directly observable from the optical/UV disc continuum. The poorly understood compton components can then be constrained by energy conservation. Assuming the soft compton and high energy corona are produced close to the black hole (as they have faster variability than seen in the disc) means that they must be powered by the accretion energy below some radius R_{cor} and that this energy can no longer be used to power the standard disc (Done et al 2012). The standard broad line AGN require $R_{cor} \sim 40R_g$ i.e that over half the accretion power is dissipated in the compton components (Jin et al 2012; Done et al 2012).

By contrast, the SEDs of 'simple' Narrow Line Seyfert 1s (NLS1) - as opposed to 'complex' NLS1 like 1H0707-495 which show dramatic X-ray variability and strong Fe K α features in their spectra (Gallo 2006) - do not look like the very high state. They look instead like the disc dominated state, with a strong disc component, weak soft X-ray excess and weak and steep coronal tail. Fitting to the energy conserving accretion models gives $R_{cor} \sim 10 - 15R_g$ (Jin et al 2012; Done et al 2012). Thus the match between unobscured AGN spectral types and BHB spectral states is not as expected for the bright AGN (Fig 1).

However, even though the NLS1 spectra look like the disc dominated BHB, the variability does not scale. The high frequency break in AGN power spectra depends on both mass and mass accretion rate (McHardy et al 2006). BHB show no real sign of this. The high/soft state in Cyg X-1 at $L/L_{Edd} \sim 0.02$ as high frequency break at ~ 10 Hz, but so do most of the power spectra of GRS1915+105 at $L \sim L_{Edd}$ - except for some which break at even lower frequencies - (Zdziarski et al 2005). The one exception is a radio quiet state identified by Trudolyubov (2001), where the noise extends up to 80-100 Hz but only at very reduced level (breaking from a flat top in $fP(f)$ at 0.001 rather than the usual 0.01).

We show an explicit comparison of the variability at $L \sim L_{Edd}$ from a 'simple' NLS1 PG1244+026, with a disc dominated state in GRS1915+105. We select a spectrum of GRS1915+105 which has similar relative strength of all the components - including a soft compton component which is apparent in this source (Fig 2) - see Middleton et al (2006) for a discussion of how this affects the derived black hole spin). Comparing bandpasses where there are similar contributions from these three components shows that 7-15 keV in GRS1915+105 corresponds to 0.3-1 keV in PG1244+026 (Fig 2). The power spectrum of GRS1915+105 (Fig 2) shows clearly that the variability increases with energy in GRS1915+105, as it does also in PG1244+026 (Fig 2). However, scaling the 0.3-1 keV power spectrum of PG1244+026 down in frequency by the $\sim 10^6$ difference in black hole mass gives a high frequency break which is

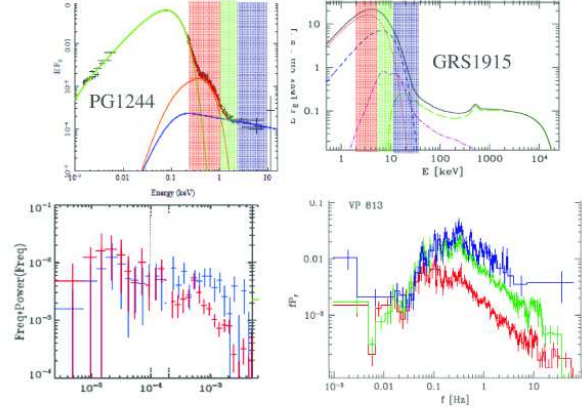


Fig. 2. Top left: The spectra of PG1244+026, which has $L/L_{Edd} \sim 1$ and $M \sim 10^7 M_\odot$ from Jin et al 2012. Top right: the spectrum of GRS1915+105: VP813 from Fig 8b in Zdziarski et al 2005. Bottom left: power spectra of PG1244+026 for 0.3-1 keV (red) and 2-10 keV (blue) from Fig 4 of Jin et al 2013. Bottom right: power spectra of GRS1915+105 for 2-7 keV (red) 7-15 keV (green) and 15-60 keV (blue). Both sources have spectra which can be decomposed into a disc, soft compton and high energy component. Both sources show variability increasing with energy, as expected if the disc is at larger radii than the soft compton, which is at larger radii than the high energy component.

a factor 30 higher than that seen for the 7-15 keV power spectrum in GRS1915+105 (Fig 3).

Thus it is clear that simply scaling BHB to AGN does not fully describe the behaviour of AGN, in terms of both their spectra and their variability. The most obvious change between BHB and AGN is the increase in mass, which leads to a decrease in temperature. AGN temperatures are then typically in the UV, and UV line driving could be an important physical mechanism in terms of setting (or disrupting) the disc structure in AGN (e.g. Proga & Kallman 2004; Risaliti & Elvis 2010). More subtly, the increase in mass means that AGN discs are more radiation pressure dominated than those in BHB as the ratio of radiation to gas pressure $\propto (\dot{m}M)^{1/4}$ (e.g. Laor & Netzer 1989). This could be important if it sets the saturation level of the MRI turbulence (Blaes et al 2013) or leads to turbulent Comptonisation in the disc (Socrates et al 2005).

3.1. Higher Order Variability techniques

Whatever the origin of the proportionally faster variability in AGN, it offers an opportunity to probe the source structure on the smallest size scales. This is especially the case as sophisticated tools for examining the spectral variability have recently been developed which go beyond simply fitting the spectra (losing all timing information) or power spectrum (losing all energy information). The new tools look at how the variability at one energy is correlated with variability at another. This can depend on

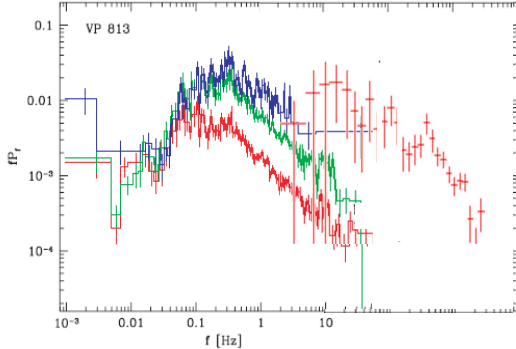


Fig. 3. An overlay of the 0.3-1 keV power spectrum of PG1244+026, scaled down in frequency by the mass difference ($14/10^7$). Clearly there is much more high frequency variability in the AGN, with the high frequency break in PG1244+026 being a factor 30 higher in frequency than expected.

frequency of variability, so requires that each lightcurve is split into its fourier components. The correlation (a measure of how coherent the two lightcurves are) as a function of fourier frequency is termed coherence, while the lags function of frequency is termed lag-frequency (Nowak et al 1999).

The recent key breakthrough has been the observation that the lag-frequency typically switches from hard lags at low frequency to soft lags at high frequency (Fabian et al 2009 as first suggested by Papadakis et al 2001; Vaughan et al 2003; McHardy et al 2004 and now seen in multiple objects: Emmanoulopoulos et al 2011; De Marco et al 2013). The soft lags indicate that some part of the soft band spectrum follows the hard X-ray variability. This is as expected in a scenario where reflection and/or reprocessing of hard X-ray illumination of the disc contributes to the soft X-ray bandpass.

Other spectral-timing products include the covariance spectra (Wilkinson & Uttley 2009). This is the spectrum of the variability which is correlated with the lightcurve in a given reference energy band. This can be made frequency dependent by selecting only a given set of fourier frequencies to include in the reference lightcurve. Similarly, the lag-energy spectra are produced by selecting a frequency range of variability, and plotting the average lag of each energy band with respect to the reference band lightcurve.

With so many new features to explore, it is now possible to try to break the multiple degeneracies in spectral fitting. Very different spectral models can fit the data e.g. comptonisation or highly smeared, reflection dominated models for the soft X-ray excess. These predict different correlations between the energy bands, so give dif-

ferent correlation based spectral-timing signatures. Any successful model must fit not just the spectrum, but the power spectrum, coherence and lag-frequency, together with the lag-energy and covariance spectra.

4. Example using PG1244+026

We use these new spectral-timing techniques to break the spectral degeneracies in fitting the simple NLS1 PG1244+026. This shows the now ubiquitous switch in lag-frequency, from soft leading at low frequencies to soft lagging at high frequencies, but this signature must be stronger/cleaner than in most AGN since it is easily detected in only 120ks of data (Alston et al 2014; Kara et al 2014 rather than the more typical 500ks in de Marco et al 2013). All details are in Gardner & Done (2014).

4.1. Soft compton model for the soft X-ray excess

We first take the model with disc, low temperature Compton component for the soft excess, high energy coronal emission for the high energy power law, and its moderately ionised, moderately smeared, moderate solid angle of reflection (Fig 4a). The soft lightcurve has less high frequency variability than the hard band, so we set up the components in a propagating accretion flow (Arevalo & Uttley 2006) with slow variability in the disc, which modulates medium variability in the soft compton, which modulates fast variability in the corona, as expected if these regions are progressively closer to the black hole (Fig 4b). We design these so that we roughly match the observed power spectra in a soft (0.3-1 keV) and hard (1.4-4 keV) energy bands (red and blue shaded areas in Fig 4c).

We include reflection on the disc (from $12-20R_g$) via a transfer function from the high energy Comptonisation component. This means that the reflected component has the same power spectrum as the high energy Compton component at low frequencies, but above 10^{-4} Hz the lags from the light travel time suppress the variability (magenta power spectra in Fig 4b). The propagation time delays (crosses on the lag-frequency plot in Fig 5a) match the low frequency soft lead seen in the data (grey shaded area). However, the model fails to reproduce the negative lag signature (ie soft lagging behind the hard) seen at high frequencies as the contribution of reflection to the soft band lightcurve is not large enough.

Instead, the negative lags can be reproduced by including the photons irradiating the disc which are *not* reflected. These instead are absorbed in the disc, heating it, and this reprocessed thermal emission adds to the soft X-ray bandpass (the disc and soft X-ray excess). This reprocessed (rather than reflected) emission does contribute enough to the soft band to make the switch between soft leading at low frequencies and soft lagging at high frequencies (filled circles in Fig 5b), and it is an

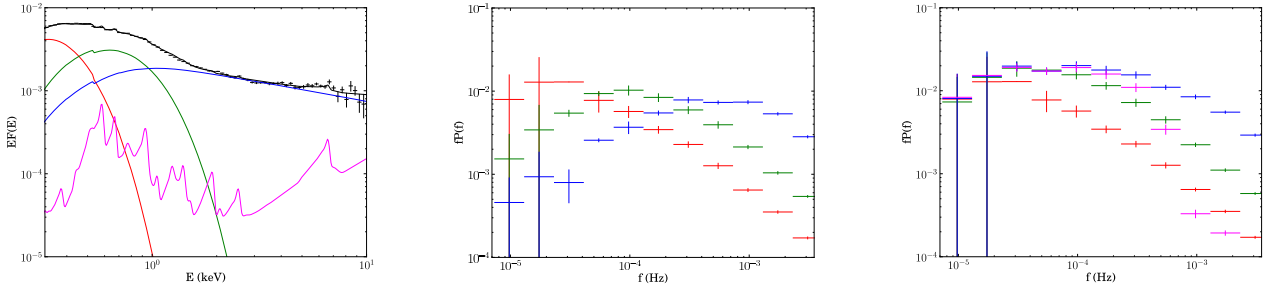


Fig. 4. a) Spectral decomposition of PG1244+026 into disc (red), low temperature Comptonised soft X-ray excess (green), high energy Compton tail (blue) and its reflection from a moderately ionised disc which subtends a solid angle of $\Omega/2\pi \sim 0.7$ with an inner radius of $12R_g$. b) the intrinsic power spectra of each component. The disc (red) is a Lorentzian centred at 3×10^{-5} Hz, while the soft X-ray excess is centred at 10^{-4} Hz (green). The high energy corona is modelled by two Lorentzians at $f_{p,1} = 3 \times 10^{-4}$ Hz and $f_{p,2} = 1 \times 10^{-3}$ Hz. c) The propagated power spectra. The disc variability (red) smoothed and lagged by 1000 s multiplies the soft X-ray excess to give the total variability of the soft X-ray excess (green) and this modulates the intrinsic coronal variability with a propagation time of 600 s, to give the total variability in the high energy Compton component (blue). This reflects from the disc (assumed to extend between $20 - 12R_g$ i.e with mean light travel time of 500 s) to give the variability in the reflected spectrum (magenta).

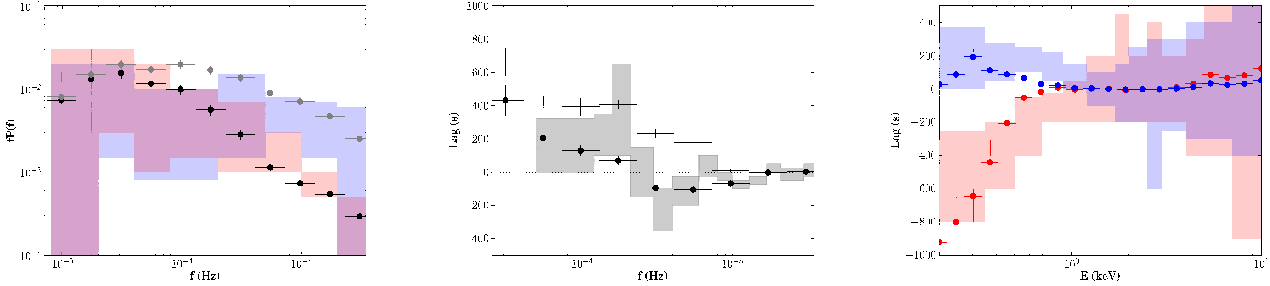


Fig. 5. a) The soft (0.3-1 keV: black) and hard (2-10 keV: grey) band power spectra resulting from the spectral-variability model of Fig 4. b) The resulting lag-frequency (crosses) compared to the observed data (grey shaded area) where soft is now 0.3-0.7 keV and hard is 1.2-4 keV. The model matches the soft lead at low frequencies from the propagation, but the contribution of reflection to the soft band is insufficient to match the negative lags seen in the data at high frequencies. Including reprocessing (thermalisation of the illuminating photons on the disc which are not reflected) can match all aspects of the observed lag-frequency (filled circles). c) The lag-energy spectra relative to a 1.2-4 keV reference band at low (red) and high (blue) frequencies from the model including reprocessing (filled circles) also matches the data (red and blue shaded areas).

inevitable physical consequence of having some reflected emission present in a fairly low mass/high mass accretion rate AGN (Gardner & Done 2014). This also matches the low and high frequency lag-energy spectra (Fig 5c).

4.2. Extremely smeared reflection for the soft X-ray excess

The extremely smeared, large solid angle reflection dominated models can also fit the spectrum (Jin et al 2013; Kara et al 2014). In these models the disc extends all the way down to the last stable orbit around a high spin black hole, and the hard X-ray source is a lamppost on the black hole spin axis. As the source height decreases, a larger fraction of the continuum power is captured by the black hole, and lightbending and the blueshift of light falling down onto the disc both boost the observed reflected spectrum compared to the observed continuum (e.g. Fabian et al 2009). This results in the innermost ring of the disc being intensely illuminated (high emissivity), so that the reflection is very strongly smeared

so that the characteristic atomic features of partially ionised material are not apparent (e.g. Crumney et al 2006).

These alternative reflection dominated models can easily match the negative lags at high frequency, but struggle to match the soft lead at low frequency. Including a power law soft component (green: Fig 6a and b) helps if this is connected to the accretion flow rather than the jet (as the jet should lag rather than lead), but a power law will contribute also to the hard X-ray band. Both soft and hard band then contain rather similar amounts of the same components so their variability is well correlated. Even the reflection component (magenta: Fig 6a and b) is well correlated as it is produced from very small radii in these models so it varies quickly. This makes it very difficult to match the drop in variability power in the soft band (black: Fig 6b) compared to the hard (grey: Fig 6b). The low frequency lag-energy spec-

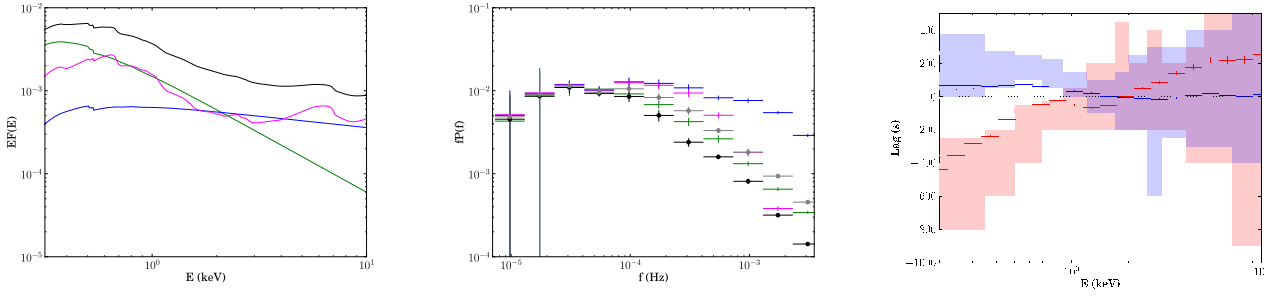


Fig. 6. a) Reflection dominated model, including a separate soft power law (green), together with a hard power law (blue) and its reflected emission (magenta) from a disc which subtends a solid angle of $\Omega/2\pi \sim 3$ and centrally concentrated emissivity for a disc with inner radius $3R_g$ ($1.4R_g$ in Kara et al 2014). b) the power spectra assuming the soft component (green) is from the accretion flow with intrinsic variability of two Lorentzians at 3×10^{-5} and 10^{-4} Hz. This propagates into the hard power law (blue) with a lag of 1200 s, modulating the intrinsic hard variability peaked at 3×10^{-4} and 10^{-3} Hz. This reflects from the disc from $1 - 12R_g$ (magenta). The soft (black) and hard (grey) power spectra are too similar to each other to match the data. c) The low frequency lag-energy spectra have a power law shape, with lag systematically increasing with energy. This is unlike the data which scatter around zero lag above 2 keV.

tra (Fig 6c) also clearly show their origin in a power law component, whereas the data (though with large error bars) are scattered around zero lag above 2 keV (Gardner & Done 2014).

5. Conclusions

Both spectra and timing properties of bright ($L/L_{Edd} > 0.02$) AGN are different from those expected from scaling bright (steady state $L/L_{Edd} > 0.02$) BHB. All the bright AGN have a soft X-ray excess which is not generally seen in BHB, and the high L/L_{Edd} AGN have substantially more variability than seen in comparable L/L_{Edd} BHB even with careful matching of emission components. Using this variability to probe the structure of the soft X-ray excess supports this being an additional component rather than extremely smeared reflection, though some of this emission must be reprocessed from the hard X-ray illumination in order to produce the soft lags seen at high frequencies. We suggest UV line driven disc winds and/or radiation pressure may be the underlying cause of the difference between BHB and AGN.

References

Alston W., Done, Vaughan, 2014, MNRAS, 439, 1548
 Arevalo P., & Uttley P., 2006, MNRAS, 367, 801
 Axelsson M., et al., 2014, MNRAS, 438, 657
 Belloni T., et al 2005, A&A, 440, 207
 Blaes O., 2013 2013 SSRv (arXiv:1304.4879)
 Boroson T., 2002, ApJ, 565, 78
 Crummey J., et al 2006, MNRAS, 365, 1067
 De Marco B., et al 2013 MNRAS 431 2441
 Done C., & Kubota A., 2006 MNRAS 371 1216
 Done C., Gierlinski, & Kubota, 2007 A&ARv 15 1
 Done C., et al., 2012, MNRAS, 420, 1848
 Elvis M., et al 1994 ApJS 95 1
 Emmanoulopoulos D., et al., 2011, MNRAS, 416, L94

Fabian A., et al 2009, Nature, 459, 540
 Gallo L. C., 2006, MNRAS, 368, 479
 Gardner E., & Done C., 2014 (arXiv:1403.2929)
 Gierlinski M., & Done C., 2004 MNRAS 349 7
 Ingram A., Done C., 2012, MNRAS, 419, 2369
 Jin C., Ward M., Done C., 2012, MNRAS, 425, 907
 Jin C., Done, Middleton, Ward, 2013, MNRAS, 2492
 Kara E., et al 2014 MNRAS 439 26
 Kotov O., et al 2001 MNRAS 327 799
 Laor A., & Netzer H., 1989 MNRAS 238 897
 Machida M., et al 2006 PASJ 58 193
 Matt G., et al 2014 MNRAS 439 3016
 Maoz D., 2007 MNRAS 377 1696
 Mayer M., & Pringle J., 2007 MNRAS 376 435
 McHardy I., et al 2004 MNRAS 348 783
 McHardy I., et al 2006 Nature 444 730
 Mehdipour M., et al 2011 A&A 534 39
 Meier D., 2005 Ap&SS 300 55
 Meyer F., & Meyer-Hofmeister E., 1994 A&A 288 175
 Middleton M., et al 2006 MNRAS 373 1004
 Miyamoto S., & Kitamoto S., 1989 Nature 342 773
 Nemmen R., et al 2014 MNRAS 438 2804
 Nowak M., et al 1999 ApJ 510 874
 Papadakis I., et al 2001 ApJL 554 133
 Proga D., & Kallman T., 2004 ApJ 616 688
 Remillard R., & McClintock J., 2006 ARA&A 44 49
 Risaliti G., & Elvis M., 2010 A&A 516 89
 Socrates A., et al 2004 ApJ 601 405
 Tamura M., et al 2012 ApJ 753 65
 Trudolyubov S., 2001 ApJ 558 276
 Vasudevan R., & Fabian A., 2007 MNRAS 381 1235
 Vaughan S., et al 2003 MNRAS 345 1271
 Wilkinson T., & Uttley P., 2009 MNRAS 397 666
 Woo J-H., & Urry M., 2002 ApJ 579 530
 Yamada S., et al 2013 PASJ 65 80
 Zdziarski A., et al 2005 MNRAS 360 825